NREL/TP-257-4508 • UC Category: 261 • DE92001159

A Comparison of Predicted and Observed Turbulent Wind Fields Present in Natural and Internal Wind Park Environments

N.D. Kelly
A.D. Wright

Prepared for Windpower '91
Conference and Exposition,
Palm Springs, California,
September 24-27, 1991

National Renewable Energy Laboratory
1617 Cole Boulevard
Golden, Colorado 80401-3393
A Division of Midwest Research Institute
Operated for the U.S. Department of Energy
Under Contract No. DE-AC02-83CH10093

October 1991

On September 16, 1991, the Solar Energy Research Institute was designated a national laboratory, and its name was changed to the National Renewable Energy Laboratory.

NOTICE

Printed in the United States of America
Available from:
National Technical Information Service
U.S. Department of Commerce
5285 Port Royal Road
Springfield, VA 22161

Price: Microfiche A01
Printed Copy A03

Codes are used for pricing all publications. The code is determined by the number of pages in the publication. Information pertaining to the pricing codes can be found in the current issue of the following publications which are generally available in most libraries: *Energy Research Abstracts (ERA)*; *Government Reports Announcements* and Index (*GRA* and I); *Scientific and Technical Abstract Reports (STAR)*; and publication NTIS-PR-360 available from NTIS at the above address.

A COMPARISON OF PREDICTED AND OBSERVED TURBULENT WIND FIELDS PRESENT IN NATURAL AND INTERNAL WIND PARK ENVIRONMENTS

N.D. Kelley
A.D. Wright

National Renewable Energy Laboratory
(formerly the Solar Energy Research Institute)
Golden, Colorado

ABSTRACT

This paper assesses the accuracy of simulated wind fields for both the natural flow and that within a wind park environment. The simulated fields are compared with the observed ones in both the time and frequency domains. Actual measurements of the wind fields and the derived kinematic scaling parameters upwind and downwind of a large San Gorgonio Pass wind park are used. The deviations in the modeled wind field from the observed are discussed.

INTRODUCTION

The ability of numerical simulations to accurately model the dynamic response of wind turbines is dependent on the credibility of the process used to generate the three-dimensional (3-D), turbulent wind field. These methods generally invoke one of several spectral and spatial coherence models. They are calculated for a single point in space using a limited number of scaling parameters as input. The simulated turbulent wind field is then constrained by the assumptions associated with the particular model employed.

Several models exist that simulate the turbulent wind inflow to both horizontal (HAWT) and vertical axis (VAWT) wind turbines. These models can be grouped into two general categories. One group simulates the inflow on a rotating blade [1-4]. The other generates a full spatial distribution of the time-varying, streamwise wind component, and the rotational field is then derived from the full-field simulation by sampling [5]. Veers [6] has recently simplified his original full-field simulation for HAWT applications by modeling the wind field at a finite number of points at the moment of blade passage. An excellent overview of the simulation codes is available in Walker, *et.al.* [7].

Up to now, the verification of these codes has been very limited. The performance of four of the readily available codes has been recently compared using a single, common inflow/turbine response data set in [7]. There has been, however, no systematic study of the ability of codes to reproduce a realistic turbulent inflow over a range of atmospheric conditions. It is important that the modeled wind fields adequately stimulate the dominant dynamic processes in wind turbines. Further, the studies that have been conducted have only used a limited range of naturally occuring flows. Flows present within a large wind park have not been examined in any detail. In this paper we address the issue of the ability of one of the simulation codes to produce a turbulent wind field in both natural and internal wind park environments, *and* over a range of atmospheric conditions.

THE CHOICE OF SIMULATION CODE

The choice of the turbulent wind simulation code to be used for this study was clear. As mentioned previously, the rotational codes model the inflow in the rotating frame of reference of the wind turbine blade. This makes validation of the turbulent wind field structure difficult with tower-based measurements unless a full, circular array of anemometers is employed. The most common approach is to compare the predicted cyclic turbine blade loads with those observed. This simulation technique, while providing some level of confidence, may not completely address the full impact of the 3-D turbulent structure.

The full-field simulation method is well suited for model verification because it can create a representative turbulent wind time series at several arbitrary locations in a reference rotor plane. It is precisely this attribute that led us to choose the Sandia HAWT simulation code (SNLWIND) [6] for our comparisons. This code has, as one of its key advantages, the ability to generate multiple blade station turbulence as an input to dynamic simulations. The code, at present, only models the streamwise or axial wind component.

COMPARISON APPROACH

The objective of this study has been to compare both the statistical and spatial structure of the simulated streamwise wind field with ensemble-averaged measured wind fields. This approach is different from previous validations where an ensemble-averaged model simulation was compared with an observed data set. The model was initiated with parameters that have been directly measured over a range of atmospheric conditions in both the natural inflow to a large wind park and in its lee. The model was configured using the Sandia-

recommended formulations, i.e., the Solari models [8]. The multiple-run random spectral and coherence features of this model, however, were not used. The Sandia model requires as inputs the: 10m mean wind speed; power law coefficient, α; surface roughness length, z_o; and coherence decrement, b.

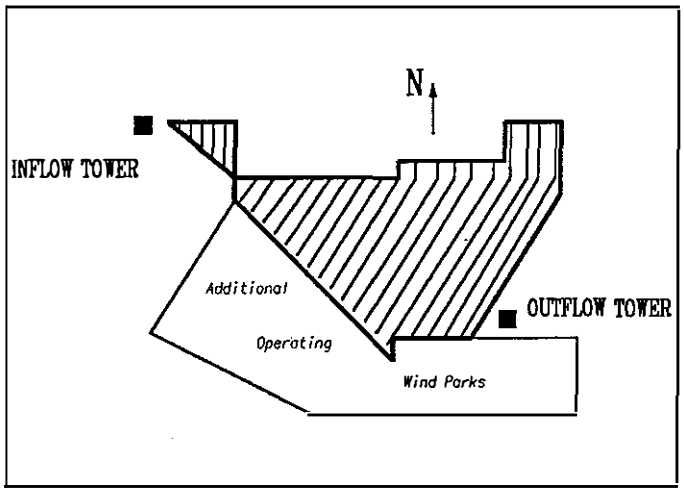

Figure 1. Schematic layout of SeaWest San Gorgonio wind park and SERI measurement tower locations.

THE REFERENCE INFLOW MEASUREMENTS

The reference measurements were collected at the 41-row SeaWest wind park located immediately east of San Gorgonio Pass in Southern California. Two 50-m micrometeorological towers were installed upwind of Row 1 (Inflow Tower) and downwind of Row 41 (Outflow Tower) as sketched in Figure 1. The turbulence regimes found at these two locations are discussed in [9].

The measurement complement on each tower consisted of cup anemometers and direction vanes at elevations of 5, 10, 20, and 50 m and a three-axis sonic anemometer at the nominal hub height of 23 m. Dry-bulb and dewpoint temperatures were measured at the 5-m elevation while the temperature difference was determined between the 5- and 50-m levels. In addition, the barometric pressure and global insolation were also recorded. The three velocity components from the sonic anemometer were recorded at 50 samples per second. The wind speeds and directions from the cups and vanes were sampled at 5 samples per second. Once per second logging was performed on the temperatures, barometric pressure, and insolation. Data were collected from the Inflow Tower for two, 2-week periods in late June and early August of 1989. A continuous record from the Outflow Tower was made for the 8-week period bracketing the Inflow Tower recording periods. Automatic system calibrations were performed at noon local standard time each day.

The resulting data volume from each tower was broken down into 10-minute records, and a series of derived parameters were calculated from those subsets. Statistical summaries were then generated for each. Using these summaries, each 10-minute record was classified by the mean 23-m wind direction, wind speed, and vertical stability. A resolution of 10 degrees was used for the wind direction and 2 ms^{-1} for the wind speed. The vertical stability was stratified into seven categories based on the value of the gradient Richardson number, Ri, defined by

$$Ri = (g/\Theta_m) \cdot (\partial\Theta/\partial z)/(\partial U/\partial z)^2$$

where g is the gravity acceleration, Θ the potential temperature given by $\Theta=T(1000/p)^{.286}$, Θ_m the mean Θ of the layer Δz, T the air temperature, p the barometric pressure, U the mean horizontal wind speed, and z the elevation height. The seven classification ranges are as follows:

(*01*) Very Unstable, (Ri < -1.0);

(*02*) Unstable, (-1.0 ≤ Ri ≤ -0.01);

(*03*) Near-Neutral, (-0.01 < Ri < +0.01);

(*04*) Critically-Stable, (+0.01 ≤ Ri ≤ +0.16);

(*05*) Stable, (+0.16 < Ri ≤ +0.25);

(*06*) Very Stable, (+0.25 < Ri +1.0); and

(*07*) Extremely Stable, (+1.0 < Ri).

A total of 464 and 937 hours of data were collected at the Inflow and Outflow Towers respectively when the 23-m mean wind speed equaled or exceeded 3 ms^{-1} (13 mph). About one-third of the total records fell into each of the stability classes 02 (unstable), 03 (near-neutral), and 04 (critically-stable) for both towers. It was necessary to use 30-minute records to assess the low-frequency contributions to the frequency spectra and vertical coherence of the streamwise wind component. This was accomplished by combining three contiguous 10-minute records when their three classifications (i.e., wind direction, wind speed, and stability) did not change. Further, these combined data sets were limited to periods when both towers were operating simultaneously and the hub-height mean wind speed equaled or exceeded 7 ms^{-1} (15 mph). This provided a data base of 819 30-minute records for the Inflow Tower (natural regime) and 641 30-minute records for the Outflow Tower (internal park regime).

The 30-minute records were used to compute the low-frequency contribution to the spectrum of the streamwise wind component. The coherence was calculated for 9 of the 10 combinations of vertical height differences. The coherence decrement b, based on the decaying exponential,

$$Coh_u(z) = \exp[-b(f\Delta z/U)],$$

Table 1. Summary of measured flow conditions used for model comparisons.

Case Code	Number 30-min Records Averaged	10m[a] Wind Speed (ms^{-1})	Power[a] Law Coef α	Surface[a] Roughness Length, z_o (m)	Coher[#] Decrmnt $b^{\#}$	23m Wind Speed (ms^{-1})	23m Speed σ_H (ms^{-1})	Ri No	Integral Scale L_u (m)
UNSTABLE INFLOW									
IST2WS4	14	6.98	0.102	0.001	4.88	7.60	1.89	-0.076	76.1
IST2WS7	88	12.25	0.113	0.002	10.59	13.50	2.78	-0.044	66.1
IST2WS9	7	16.04	0.126	0.004	13.37	17.65	3.83	-0.027	44.5
UNSTABLE OUTFLOW									
OST2WS4	38	7.01	0.147	0.044	6.68	7.39	3.19	-0.080	27.7
OST2WS7	16	12.40	0.146	0.028	12.01	13.34	4.62	-0.037	40.8
OST2WS9	2	15.10	0.156	0.041	12.23	16.84	4.32	-0.035	18.2
NEAR-NEUTRAL INFLOW									
IST3WS4	1	7.42	0.103	0.002	5.25	8.21	1.30	+0.002	25.5
IST3WS7	54	12.01	0.154	0.020	10.00	13.54	2.58	+0.003	57.0
IST3WS9	69	15.53	0.151	0.017	13.79	17.43	2.70	+0.003	55.7
NEAR-NEUTRAL OUTFLOW									
OST3WS4	6	7.06	0.159	0.071	7.42	7.47	3.43	+0.001	68.3
OST3WS7	57	12.46	0.159	0.063	12.24	13.53	3.72	+0.005	36.5
OST3WS9	11	15.36	0.163	0.063	13.98	17.15	4.61	+0.004	80.9
CRITICALLY-STABLE INFLOW									
IST4WS4	23	6.86	0.149	0.034	4.85	7.67	1.90	+0.056	83.9
IST4WS7	70	12.03	0.143	0.018	10.04	13.42	2.43	+0.017	63.3
IST4WS9	3	15.34	0.180	0.045	13.57	17.72	2.01	+0.013	64.8
CRITICALLY-STABLE OUTFLOW									
OST4WS4	61	6.80	0.177	0.140	6.38	7.46	2.65	+0.041	24.1
OST4WS7	3	12.08	0.159	0.062	12.93	13.14	3.92	+0.012	46.5

[a]Model input parameters [#]Based on *coherence-squared* function

was calculated from these nine values of Δz. The results were then smoothed with a robust, locally weighted smoothing routine [10]. In addition to the coherence decrement, the power law coefficient, α, and the surface roughness length, z_o, were calculated from the five-level mean wind profile. The high-frequency portion of the streamwise wind component (u) was calculated from the sonic anemometer, which has a maximum frequency response of 10 Hz. The low-frequency portion of the sonic u-spectrum was then combined with that from the high-frequency range to form a wideband spectral estimate covering an overall frequency band of .00315 to 10 Hz (periods of 0.1 to 317 s).

A series of subsets were defined by averaging the model input parameters for all *westerly* wind direction classes with wind speed classes 04 (8±1 ms^{-1}), 07 (14±1 ms^{-1}), and 09 (18±1 ms^{-1}). These wind speed classes correspond to near cut-in, rated, and above-rated operations for many wind turbines. To define the model cases to be evaluated, a matrix was constructed using these wind direction/speed combinations with the three stability classes found to contain the bulk of the data above 7 ms^{-1} (classes 02, 03, and 04). This combination of three stability and three mean wind speed classes results in a maximum of nine cases for model comparison. Table 1 lists the ensemble mean input parameters for each of these cases and four additional parameters of interest: the 23-m (hub) mean wind speed, the 23-m *total horizontal* wind speed standard deviation σ_H, the Richardson number, and the mean *longitudinal* integral scale L_u. There are only eight cases for the Outflow Tower since there were no observed records with a wind speed class of 09 and stability class of 04. The table also lists the number of 30-minute records used to produce the mean quantities shown.

MODEL CONFIGURATION

The Sandia model was configured for two sets of simulations. One was used to simulate wind fields at the height of the five SERI tower anemometers at a rate of twice per second. The other simulated the sonic anemometer at a rate of 20 per second. The low-rate data was created by specifying a two-bladed rotor with four radial stations and hub height. A time series of 8,192 points was generated by requesting a rotation rate of once per second and two points per rotation. The resulting time series were truncated to 7,200 points (30-minutes at twice per second) before analyzing the simulated data.

Table 2. Comparison of measured and modeled bulk parameters.

Case Code	Obs u_{*_o} (ms^{-1})	Model u_{*_m} (ms^{-1})	Obs 23m σu_o (ms^{-1})	Model 23m σu_m (ms^{-1})	Obs Coher Dec[b] b_o	Model Coher Dec[b] b_m	Obs Peak Gust[a] (ms^{-1})	Model Peak Gust[a] (ms^{-1})
UNSTABLE INFLOW								
IST2WS4	0.286	0.286	1.12	0.76	4.88	5.03	11.9	10.5
IST2WS7	0.550	0.565	1.68	1.48	10.59	12.49	23.5	19.0
IST2WS9	0.788	0.835	2.18	2.13	13.37	14.97	26.6	25.6
UNSTABLE OUTFLOW								
OST2WS4	0.504	0.425	2.13	1.25	6.68	7.91	25.4	12.8
OST2WS7	0.843	0.752	3.10	2.15	12.01	15.01	43.6	22.0
OST2WS9	1.096	0.988	2.62	2.76	15.10	13.25	43.9	27.3
NEAR-NEUTRAL INFLOW								
IST3WS4	0.308	0.307	0.70	0.87	5.25	5.42	9.9	10.5
IST3WS7	0.746	0.773	1.52	1.99	10.00	11.05	20.6	21.1
IST3WS9	0.932	0.980	1.61	2.53	13.79	17.09	26.8	26.9
NEAR-NEUTRAL OUTFLOW								
OST3WS4	0.575	0.469	2.23	1.34	7.42	7.88	23.5	13.2
OST3WS7	0.979	0.830	2.48	2.38	12.24	13.88	38.9	23.0
OST3WS9	1.207	1.054	3.06	2.96	15.36	14.87	47.4	28.4
CRITICALLY-STABLE INFLOW								
IST4WS4	0.414	0.424	1.00	1.20	4.85	4.92	15.2	12.3
IST4WS7	0.696	0.713	1.40	1.95	10.04	11.14	22.9	20.8
IST4WS9	1.101	1.176	1.25	2.89	13.57	16.22	21.2	28.4
CRITICALLY-STABLE OUTFLOW								
OST4WS4	0.637	0.509	1.72	1.43	6.38	7.71	29.6	13.3
OST4WS7	0.958	0.805	2.56	2.30	12.93	12.45	38.9	22.4

[a]23m height [b]Based on *coherence-squared* function

The high-frequency portion of the streamwise component (measured by the sonic anemometer) was simulated by sampling a single radial station at a rotational frequency of 20 revolutions per second. In this manner, a 16,384-point time series was generated, which was truncated to 12,000 to simulate a 10-minute record with a 10-Hz bandwidth. The model was operated with the Sandia-recommended Solari models for the turbulent spectrum and coherence. Neither of the Solari randomization features (spectra and coherence decrement) were invoked.

ANALYSIS METHODOLOGY

The simulated time series were processed and analyzed with the identical software that was used to process the observed measurements. The coherence decrement, b, was determined using a duplicate sequence as was discussed previously. A statistical summary was generated for each of the modeled runs and calculations of kinematic properties of the simulated flow such as the shear or friction velocity, u_*, were made. The objective was to measure as many of the structural flow parameters as possible to compare with actual measurements.

RESULTS

Table 2 summarizes three key kinematic properties of the actual and modeled flows: the friction velocity u_*, the standard deviation of the streamwise component σ_u, and the coherence decrement b. Also included are the observed and simulated peak gusts for each set of flow conditions.

Comparisons of the ensemble-averaged observed spectra and the model results are presented in Figures 2, 3, and 4 for the three stability classes 02 (unstable), 03 (near-neutral), and 04 (critically-stable) respectively. An example of the time-correlation of the hub-height flow for the natural flow (Inflow Tower) and park internal flow (Outflow Tower) under unstable conditions and a mean wind speed of 13.5 ms^{-1} is shown in Figure 5. The autocorrelation coefficient of the model simulation has also been plotted. The rotational

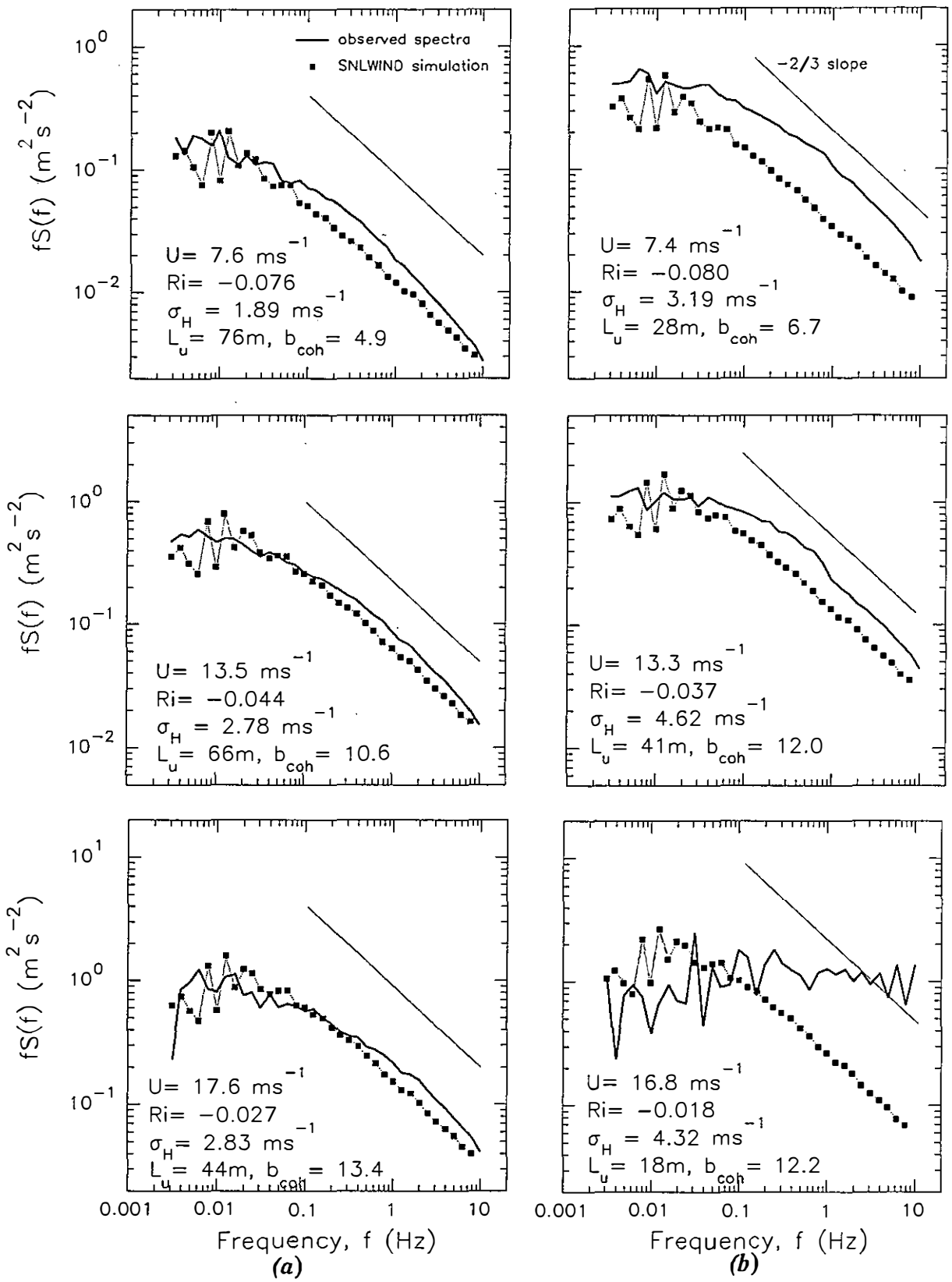

Figure 2. Comparison of simulated and observed streamwise spectra for: (*a*) inflow and (*b*) outflow unstable flow cases.

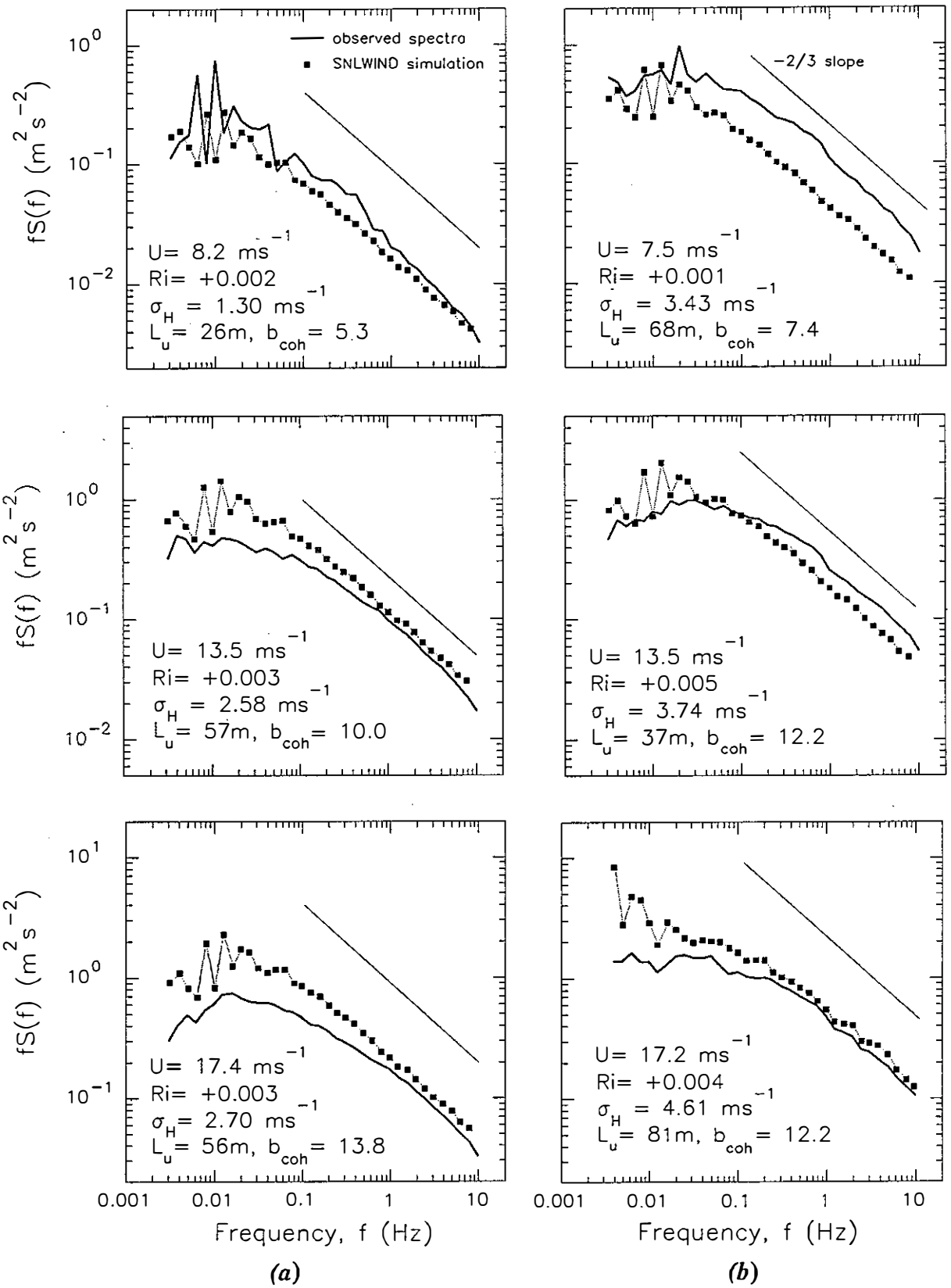

Figure 3. **Comparison of simulated and observed streamwise spectra for: (*a*) inflow and (*b*) outflow near-neutral flow cases.**

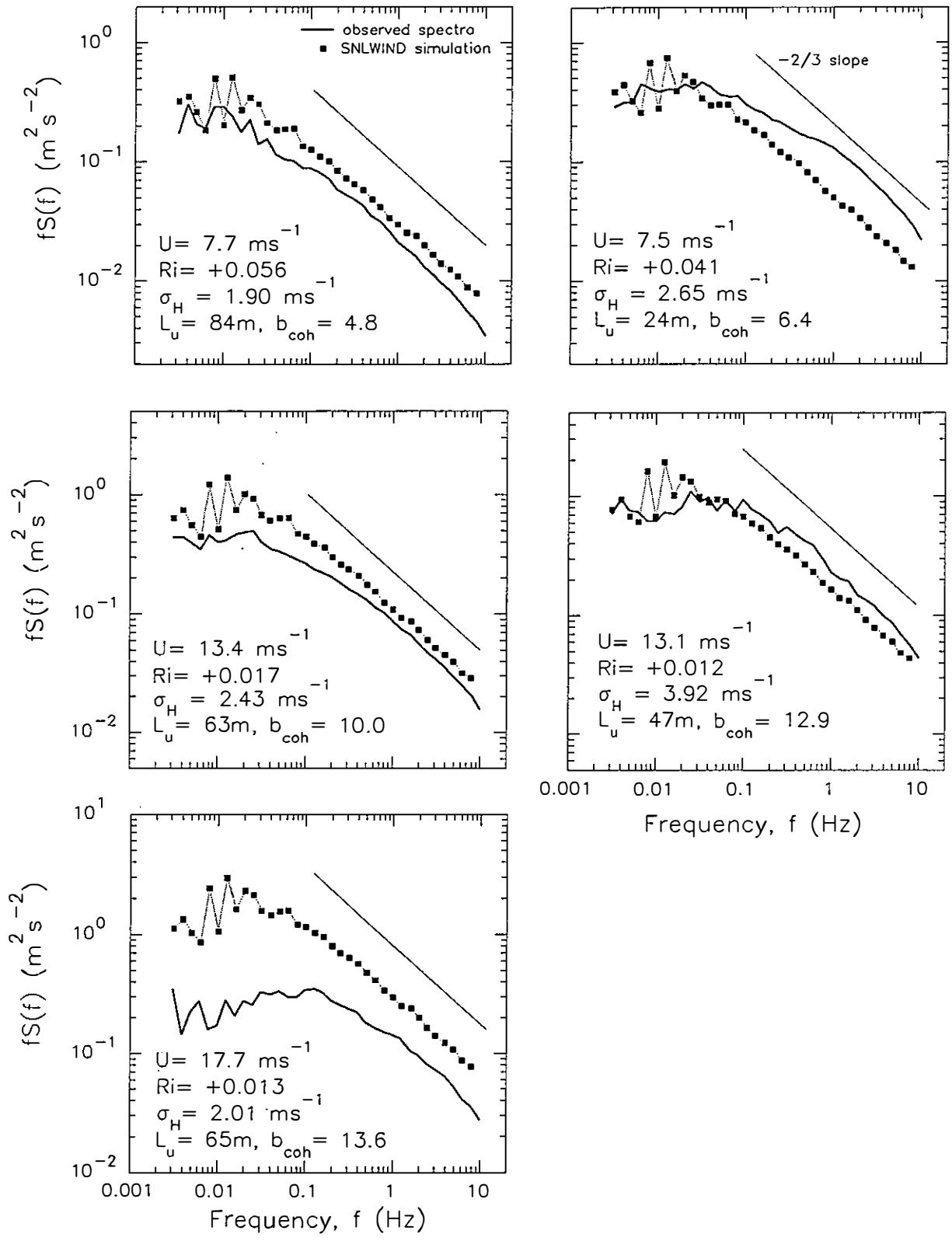

Figure 4. Comparison of simulated and observed streamwise spectra for: (*a*) inflow and (*b*) outflow critically-stable flow cases.

period of a Micon 65 turbine has been indicated for reference.

DISCUSSION

The model, when first run, produced simulated coherence decrements double those specified. This had a significant impact on the statistics of the simulated wind field and caused wide discrepancies between simulated values and observed. We traced the problem to a common one. The Solari formulation uses the ***square root*** of the coherence function as a definition. The decrements listed in Tables 1 and 2 are based on the ***coherence-squared*** function. The coherence decrements associated with the former are ***twice*** the latter.

Natural Flows (Inflow Tower)

The results in Table 2 and the spectra in Figures 2 and 3 indicate that the model does a reasonable job of simulating the streamwise component of the natural inflow for unstable and near-neutral conditions. The largest discrepancy is the over-prediction of the total turbulent energy (σ_u) in the near-neutral case. The answer may be found when one compares the ***total horizontal*** values of σ_H shown in Table 1 and on the individual spectral plots. The measured values of σ_u are significantly less the than the total horizontal σ_H suggesting the turbulent cross-wind component contains a significant amount of variance not accounted for by the model. In general, the model does a good job of simulating peak values under these conditions.

The behavior exhibited under critically stable flow conditions is to be expected because the model assumes a neutral atmosphere. Under such an assumption, one would expect the model to over predict the level of turbulence, particularly at the higher mean wind speeds. This over-prediction is evident in the spectral comparisons of Figure 4 and the Table 2 entries for the 13.5 and 17 ms^{-1} cases. The model does, however, do a good job of simulating the peak gusts.

Internal Park Flows (Outflow Tower)

In general one would not expect the model to reproduce the internal park flow as accurately as the natural flow because sources of turbulence exist (upstream turbine wakes) that it does not consider. Such a condition is plainly evident in the low-wind spectra of Figures 2, 3, and 4 and the entries of Table 2. The model under-predicts the turbulence levels in the smaller turbulent scales, which would be consistent with the contribution of the wakes. The degree of model under-prediction decreases with increasing mean wind speed. This suggests that the added wake turbulence increases the efficiency of the vertical mixing process. The Outflow spectra of Figure 2 for the case of 16.8 ms^{-1} clearly demonstrates that under strong gusts, the spectral content of the turbulent inflow is materially different from that predicted. It is also evident from Table 2 that the model cannot reproduce the extremes seen in the internal park flows.

Time-Correlated Structure

The modeled time series were applied to the codes that were used to compute the integral scales listed in Table 2. The actual flows were found to have integral time scales the order of 3 to 10 seconds and space scales less than 100 m. The model results produced time and integral scales in narrow ranges of 2 to 4 seconds and 20 to 50 m respectively for all comparison cases. Figure 5 displays the measured autocorrelations for the inflow and outflow sonic anemometer streamwise components and simulated by the model for an unstable flow case with a 13.5 ms^{-1} mean wind speed.

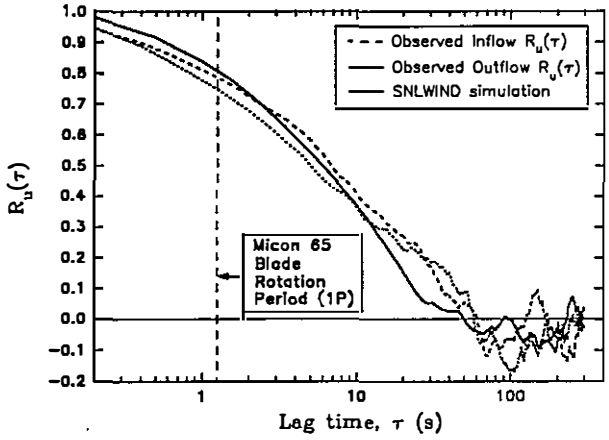

Figure 5. Comparison between measured and simulated streamwise wind component autocorrelations.

The simulated and observed integral scales as a function of stability regime and mean wind speed are summarized in Figure 6 for the natural and internal park flows. As can be seen from the figure, the model predicts turbulence regimes which are essentially independent of stability and vary only slightly with mean wind speed. The natural inflow tends to exhibit larger integral scales at lower wind speeds under non-neutral conditions. There is better agreement between the modeled scales and those observed in the outflow or internal park regime.

CONCLUSIONS

The Sandia HAWT simulation model does a good job of simulating many of the properties of the natural turbulent inflow present in San Gorgonio Pass under unstable and near-neutral stability conditions. Since it only predicts the streamwise or axial wind component, it cannot account for the substantial cross-flow or in-plane turbulent energy present in the natural wind at this location. As would be expected, it systematically over predicts the turbulent energy present in stable flows particularly at the higher wind speeds. It does a good job of simulating naturally occuring peak gusts.

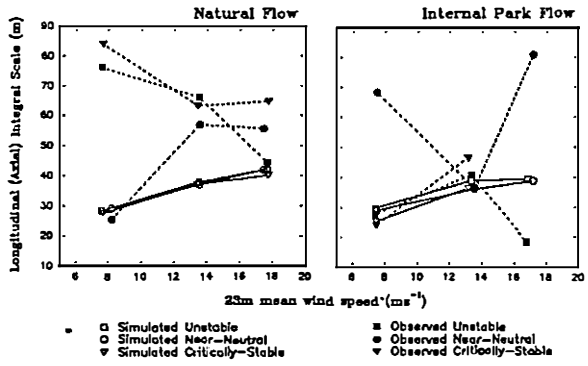

Figure 6. Comparison of modeled and observed integral scales.

As expected, the model under-predicts the small-scale turbulence levels present in internal park flows. This discrepancy becomes smaller as the wind speed and stability increase. It significantly under-predicts the observed peak gusts and the small-scale turbulent energy associated with them. The model reproduces the time-correlation properties of the axial wind component with reasonable accuracy. It may be considered to produce conservative results if integral scales approaching the dimensions of the wind turbines are shown to be important for fatigue and energy capture considerations.

It is justified to consider upgrading the code to handle non-neutral (*diabatic*) conditions considering the high percentage of time these conditions exist in a typical wind park environment. It is also justified to consider expanding the prediction to include all three velocity components to take into account the structure of winds such as are seen in San Gorgonio Pass and that may have substantial impacts on turbine component lifetimes.

ACKNOWLEDGEMENTS

This work has been supported by the U.S. Department of Energy under contract DE-AC02-83CH10093. The data to make the model comparisons discussed in this paper have been made possible by the excellent cooperation of the SeaWest Energy Group, Inc., and its Palm Springs Operation in particular. Without the dedicated efforts of Bob Keller of Sugarloaf Enterprises, Inc. and Ed McKenna, Brian Smith, Jack Allread, Dave Jager, and Doyle Selix of SERI the field data collection would not have been possible. George Scott provided the expertise to process the data and Gary Desrochers coded the locally weighted smoothing (LOESS) routine used in the coherence decrement calculations.

REFERENCES

1. Kristensen, L. and S. Frandsen, "Model for Power Spectra of the Blade of a Wind Turbine Measured from a Moving Frame of Reference," J. Wind Engr & Indust. Aero., Vol. 10, 1982.

2. Anderson, M.B., "The Interaction of Turbulence with a HAWT," Proc. 4th BWEA Wind Energy Conf., Univ. of Cambridge, 1982.

3. Connell, J.R., *et.al.*, The PNL Single-Tower Measurement Model of Rotationally Sampled Turbulent Wind, STRS2PC, Specialized for Use on an IBM-PC Computer with Users Guide, Pacific Northwest Laboratories, 1987.

4. Holley, W.E., *et.al.*, "Wind Turbulence Inputs for Horizontal Axis Wind Turbines," Proc. Wind Turbine Dynamics Workshop," Cleveland, OH, SERI/CP-635-1238, 1981.

5. Veers, P.S., Modeling Stochastic Winds on Vertical Axis Wind Turbines, SAND83-1909, Sandia Nat'l Laboratories, 1984.

6. Veers, P.S., Three-Dimensional Wind Simulation, SAND88-0152, Sandia Nat'l Laboratories, 1988.

7. Walker, S.N., T.L. Weber, and R.E. Wilson, A Comparison of Wind Turbulence Simulation Models for Stochastic Loads Analysis for Horizontal Axis Wind Turbines, SERI/STR-217-3463, Solar Energy Research Institute, 1989.

8. Solari, G., "Turbulence Modeling for Gust Loading," J. Struct. Engr, Vol. 113, 1987.

9. Kelley, N.D., "An Initial Look at the Dynamics of the Microscale Flow Field with a Large Wind Farm in Response to Variations in the Natural Inflow," Proc. Windpower '89, SERI/TP-257-3628, Solar Energy Research Institute, 1989

10. Chambers, J.M., *et.al.*, Graphical Methods for Data Analysis, Pacific Grove, California: Wadsworth & Brooks/Cole Co. (1983), 395pp.